Available online at www.sciencedirect.com
ScienceDirect
Journal of Sound and Vibration 297 (2006) 1048–1067
JOURNAL OF SOUND AND VIBRATION
www.elsevier.com/locate/jsvi

Stochastic output error vibration-based damage detection and assessment in structures under earthquake excitation

J.S. Sakellariou, S.D. Fassois*

Stochastic Mechanical Systems and Automation (SMSA) Laboratory, Department of Mechanical and Aeronautical Engineering, University of Patras, GR 26500 Patras, Greece

Received 9 February 2004; received in revised form 4 May 2006; accepted 9 May 2006
Available online 7 July 2006

Abstract

A stochastic output error (OE) vibration-based methodology for damage detection and assessment (localization and quantification) in structures under earthquake excitation is introduced. The methodology is intended for assessing the state of a structure following potential damage occurrence by exploiting vibration signal measurements produced by low-level earthquake excitations. It is based upon (a) stochastic OE model identification, (b) statistical hypothesis testing procedures for damage detection, and (c) a geometric method (GM) for damage assessment. The methodology's advantages include the effective use of the non-stationary and limited duration earthquake excitation, the handling of stochastic uncertainties, the tackling of the damage localization and quantification subproblems, the use of "small" size, simple and partial (in both the spatial and frequency bandwidth senses) identified OE-type models, and the use of a minimal number of measured vibration signals. Its feasibility and effectiveness are assessed via Monte Carlo experiments employing a simple simulation model of a 6 storey building. It is demonstrated that damage levels of 5% and 20% reduction in a storey's stiffness characteristics may be properly detected and assessed using noise-corrupted vibration signals.

1. Introduction

The problem of *damage detection* and *assessment* (the latter term signifying localization and quantification) in civil and related infrastructure, such as highway or railway bridges, buildings, dams, and so on, has been receiving increasing attention in recent years [1–4]. *Vibration-based methods* constitute a promising approach, as they are "global", in the sense of being capable of monitoring the structure's global characteristics, relatively easy to implement, and also possible to "automate". Moreover, they tend to be time effective and less expensive than most alternatives [5,6].

Abbreviations: AR, autoregressive; ARMA, autoregressive moving average; DA, dispersion analysis; GM, geometric method; N/S, noise-to-signal; X, exogenous; OE, output error; RARMA, recursive autoregressive moving average; RML, recursive maximum likelihood (method).

*Corresponding author. Tel./fax: +30 2610 997 405; 2610 997 130.
E-mail address: fassois@mech.upatras.gr (S.D. Fassois).
URL: http://www.mech.upatras.gr/~sms.

0022-460X/$ - see front matter © 2006 Elsevier Ltd. All rights reserved.
doi:10.1016/j.jsv.2006.05.009

The *fundamental principle* upon which vibration-based methods are founded is that small changes (damage) in a structure cause behavioral discrepancies in its vibration response. The goal thus is the reliable detection of such discrepancies in a structure's measured vibration response and their precise association with a specific cause (damage localization and quantification). Broadly speaking, this may be achieved by ''comparing'' a *nominal* structural model (representing the ''healthy'' structure) with a corresponding *current* model (representing the structure in its current—unknown—condition). Thus the two most important elements of a vibration-based method are (a) the structural *model* used (the term model presently used in its broadest sense), and (b) the decision-making mechanism (which uses some of the model's features) responsible for the ''comparison''.

1.1. Classification and overview of vibration-based damage detection and assessment methods

Depending upon the nature of the structural model used, the decision-making mechanism, the way of operation, and so on, vibration-based methods may be classified in various ways. For instance, depending upon the nature of the model, they may be classified as *parametric* (a parametric model is used) or *non-parametric* (a non-parametric model is used). Furthermore, when the model is identified from available vibration signals, the methods are characterized as *time series based*. Depending upon the nature of the decision-making mechanism, they may be classified as *stochastic* (statistical decision making that takes uncertainties into account is used) or *deterministic* (uncertainties are not taken into account). Depending upon their way of operation, they may be classified as *off-line* (the decision is made off-line, following damage occurrence and subsequent signal acquisition) and *on-line* (the decision is made on-line, as damage occurs).

In the following a brief overview of the main families of methods, classified according to the type of structural model used, is presented.

One family of methods utilizes ''large'' size *finite element models* and examines changes incurred in the structural model's stiffness matrix by using model updating based upon dynamic and/or static test data [7–10]. An alternative family utilizes identified *modal models*, and damage detection is based upon the assessment of changes in the characteristics of the nominal and current models [11–14]. The former methods often have the advantage of tackling the damage-assessment problem as well; this is in general harder to do with the latter. Nevertheless, both families are characterized by limitations such as the need for ''large'', detailed, structural models, a large number of sensors, elaborate testing procedures, the frequent lack of accounting for random effects and uncertainties, and so on (see, for instance, Refs. [15–17]).

Another family of methods is based upon *state-space structural models*, obtained via subspace identification techniques, and statistical decision-making [18,19]. These methods have the advantage of being capable of working on-line, and also coping with uncertainties and certain types of non-stationary excitation. This last characteristic is important as the signals measured on a civil structure are often due to earthquake or ambient (wind or traffic induced) excitation, and are known to be strongly non-stationary. Yet, the methods mainly address the damage detection subproblem (not the damage assessment, that is localization and quantification) and (unlike the present methodology) they are based upon proper model ''residuals'' for statistical fault detection (no current model is used).

Another, yet, family of methods is based upon identified *nonlinear structural models* (including artificial neural network models) and decision-making mechanisms that may use a comparison of the response error between a nominal model and the actual structure [20–22]. These methods are useful in cases of structures operating beyond their linear regime (for instance they may be experiencing damage—the on-line case). Yet, they are mainly deterministic, the models used are complicated, of ''large'' sizes, and relatively difficult to obtain, validate and physically interpret. These methods also tend to be ''sensitive'' to modelling errors.

An alternative family is based upon *non-stationary vibration models*, which are usually non-parametric wavelet-based models, and decision-making mechanisms based upon the examination of changes incurred in their characteristics [23–25]. The advantage of these methods is that they are suitable for the representation of nonlinear and non-stationary vibration, and may be appropriate for on-line use. Yet, decision making is mainly deterministic, not easy to ''automate'', and the focus usually is on the damage detection subproblem.

A final, but popular, family of methods is based upon non-parametric vibration models in the form of *damage indices* and deterministic decision-making mechanisms. These use interstorey drifts in buildings,

require measurements in every storey, and thus extensive instrumentation [26–29]. Furthermore, certain widely used damage indices, which combine the maximum deformation and the absorbed hysteretic energy, require the empirical selection of several critical values leading to methods that are not robust and without general applicability [30,31].

For a survey and further discussion of the wide category of time series type methods for general vibration-based structural damage detection and assessment the interested reader is also referred to the forthcoming publication [32].

1.2. Scope and framework of the work

This paper focuses on the *off-line* damage detection and assessment problem and specifically on the use of *low-level earthquake excitations* under which the structure stays within its *linear* operating regime. The methodology developed is thus intended for *periodically*, or after a major event with potentially harming consequences, assessing the state of a given structure.

The specific focal points and respective advantages of the methodology developed in this paper are: (i) The proper and effective use of *non-stationary earthquake excitation* (see next paragraph for more on this). (ii) The effective handling of uncertainties via *stochastic* techniques in both the structural modelling and the decision-making mechanism. (iii) The tackling of the important *damage assessment* (localization and quantification) subproblem alongside with the damage detection subproblem (that is solely treated by many alternative methods). (iv) The utilization of *simple and partial* (in both the spatial and frequency bandwidth senses) identified structural models of "*small*" *size* (small number of estimated parameters). This is in contrast to complete or "large" size (detailed) models required by many methods. (v) The requirement for a *minimal number* (even a single pair) of measured vibration signals (unlike the significant number of signals required by many methods). This simplifies the experimental procedure and the measurement set up. Naturally, an unavoidable consequence of the last two characteristics is that only *gross* (approximate) damage localization is possible.

A few words on the intended use of low-level earthquake excitation are now in order. The use of this type of excitation is motivated by the fact that the generation of artificial excitation may, especially for large structures, be difficult or expensive. Thus, "natural" excitation due to earthquake events (also traffic, strong wind, and so on) represents a useful alternative [2,23,33]. Earthquake excitation is particularly attractive in earthquake prone areas, is rich in low-frequency content, and often leads to vibration responses of a sufficient level. On the other hand, its characteristics introduce a number of technical difficulties and limitations which may be summarized as follows: (a) Its transient nature, and resulting *limited duration*, which limits the identification data record length. (b) Its *limited frequency content*, which narrows attention to the lower-frequency modes. (c) Its *non-stationarity*, in terms of both amplitude and frequency, which renders methods requiring stationary signals (like classical frequency domain methods) inappropriate (for instance see Refs. [34,35]). Coping with these characteristics requires caution and proper selections, and this is a main issue that is addressed by the present methodology.

1.3. Overview of the output error (OE) model-based methodology

The OE model-based damage detection and assessment methodology consists of the following main elements:

(a) *Stochastic OE structural modelling* via proper identification techniques. OE models (see Refs. [36, pp. 81–90; 37]) are selected as they are instrumental in overcoming the problems associated with earthquake ground motion non-stationarity. This is due to the fact that no assumptions are made on the noise corrupting the response measurements (see Section 3.2). Furthermore, their *stochastic* nature leads to proper accounting of uncertainties, and their *parametric* nature warrants high achievable accuracy and resolution even with earthquake events of limited time duration. The OE models employed are discrete time, of "small" size (few model parameters) and partial (in the sense already described). One OE model is used for representing the structure in its nominal (healthy) state, and one in its

current (unknown) state. Within the context of damage assessment additional OE models are used for representing the structure under different states of damage.

(b) *Statistical hypothesis testing procedures* for damage detection. These are based upon the identified (nominal and current) OE model parameters, and are essential for properly detecting damage at a user-specified probability level and effective decision making under experimental uncertainty.

(c) A *geometric method* (*GM*) for damage assessment (gross localization and quantification). This method has been introduced by the second author and his co-worker [16,38] for general damage localization. In this study it is, for the first time, applied to damage localization for structures under earthquake excitation, and also extended to include damage quantification.

The OE model-based methodology is demonstrated, and its feasibility and effectiveness are examined, via Monte Carlo experiments pertaining to damage detection and assessment in a simple, transversal, simulation model of a 6 storey building subject to earthquake excitation. This simulation model should not be confused with the OE models internally used by the methodology. It is a physics-based model, with its sole purpose being simulation, serving as the study's paradigm. It has been chosen to be simple for demonstrating the principles and steps of the methodology, and yet sufficient for demonstrating its effectiveness with regard to damage detection and (gross) localization.

The rest of the paper is organized as follows: The transversal simulation model of the building, along with the damage cases and the seismic excitation are presented in Section 2. The stochastic OE model-based damage detection and assessment methodology is introduced in Section 3. Monte Carlo damage detection and assessment results are presented in Section 4, and the conclusions are summarized in Section 5.

2. The building simulation model, damage cases and the excitation

The simple transversal simulation model of the building, the damage cases, and the seismic excitation used as the study's paradigm are presented in the following subsections.

2.1. The transversal simulation model of the building

A schematic representation of the lumped-parameter physics-based simulation model describing the transversal motion of a 6-storey building is shown in Fig. 1. Each storey, of dimensions $10\,\mathrm{m} \times 20\,\mathrm{m} \times 3\,\mathrm{m}$, is modelled via a lumped-parameter representation of its inertial ($m_i = 3 \times 10^5\,\mathrm{kg}$), stiffness ($k_i = 9.696 \times 10^5\,\mathrm{kN/m}$), and power dissipation ($c_i = 17.11 \times 10^5\,\mathrm{Ns/m}$) properties. The mass of each storey is assumed to be concentrated in the storey's upper region. The stiffnesses represent the complex construction of the concrete, with parts of steel and other metals. The building's transversal dynamics are thus described by the differential equation (lower/upper case bold face symbols designate vector/matrix quantities, respectively):

$$\mathbf{M}\ddot{\mathbf{x}} + \mathbf{C}\dot{\mathbf{x}} + \mathbf{K}\mathbf{x} = \mathbf{Q}\mathbf{x}_0 \tag{1}$$

with $\mathbf{x} = [x_1\ x_2\ x_3\ x_4\ x_5\ x_6]^{\mathrm{T}}$ designating the displacement vector (x_i referring to the transversal displacement of the ith storey; Fig. 1), $\mathbf{x}_0 \triangleq [x_0\ \dot{x}_0]^{\mathrm{T}}$ the input vector (x_0 referring to the transversal ground displacement), $\mathbf{Q}$ an input shaping matrix, and $\mathbf{M}$, $\mathbf{K}$, $\mathbf{C}$ the mass, stiffness, and viscous damping matrices, respectively. These quantities are of the following forms:

$$\mathbf{Q} = \begin{bmatrix} k_1 & 0 & 0 & 0 & 0 & 0 \\ c_1 & 0 & 0 & 0 & 0 & 0 \end{bmatrix}^{\mathrm{T}}, \tag{2}$$

$$\mathbf{M} = \mathrm{diag}\,(m_1, m_2, \ldots, m_6), \tag{3}$$

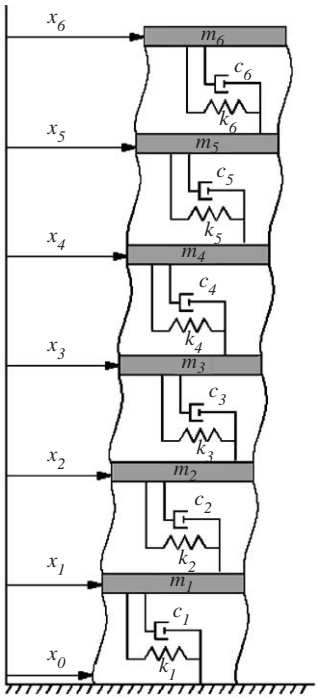

Fig. 1. Schematic diagram of the 6 storey building model.

$$\mathbf{K} = \begin{bmatrix} k_2 + k_1 & -k_2 & 0 & 0 & 0 & 0 \\ -k_2 & k_3 + k_2 & -k_3 & 0 & 0 & 0 \\ 0 & -k_3 & k_4 + k_3 & -k_4 & 0 & 0 \\ 0 & 0 & -k_4 & k_5 + k_4 & -k_5 & 0 \\ 0 & 0 & 0 & -k_5 & k_5 + k_6 & -k_6 \\ 0 & 0 & 0 & 0 & -k_6 & k_6 \end{bmatrix}, \tag{4}$$

$$\mathbf{C} = \begin{bmatrix} c_2 + c_1 & -c_2 & 0 & 0 & 0 & 0 \\ -c_2 & c_3 + c_2 & -c_3 & 0 & 0 & 0 \\ 0 & -c_3 & c_4 + c_3 & -c_4 & 0 & 0 \\ 0 & 0 & -c_4 & c_5 + c_4 & -c_5 & 0 \\ 0 & 0 & 0 & -c_5 & c_5 + c_6 & -c_6 \\ 0 & 0 & 0 & 0 & -c_6 & c_6 \end{bmatrix} \tag{5}$$

with diag(·) designating diagonal matrix.

Within the context of the present paradigm, structural damage detection and assessment are to be based upon a *single pair* of measurements (partial system information): That of the ground displacement (x_0) and the 6th storey acceleration ($\ddot{x}_6$). The theoretical modal characteristics of the continuous-time transfer function $\ddot{X}_6/X_0$, which relates the two signals and represents the corresponding dynamics, are presented in Table 1.

2.1.1. State-space formulation

The building dynamics are now set in state-space form, that is as a set of first-order differential equations. This form is used in the simulations, as it is known to be characterized by improved numerical properties

Table 1
Theoretical building characteristics ($\ddot{X}_6/X_0$ transfer function of the simulation model)

f_n (Hz)	ζ (%)	Residue
2.18	1.21	$1.0 + j0.0$
6.41	3.56	$7.647 - j0.731$
10.28	5.70	$15.227 + j1.371$
13.54	7.51	$16.992 - j2.995$
16.02	8.88	$11.732 + j1.818$
17.57	9.74	$3.698 - j0.824$

(see, for instance, Ref. [39, p.477]). Furthermore, it avoids potential numerical inconsistencies in the excitation, as, in contrast to the model of Eq. (1) where the vector $\mathbf{x}_0$ on the right-hand side includes both the ground motion displacement and velocity, only the ground displacement is used as excitation in the state-space form [see Eq. (10a)].

For converting the simulation model into state-space form the building equations of motion [Eq. (1)] may be expressed as

$$\ddot{x}_1 + \frac{k_1 + k_2}{m_1} \cdot x_1 - \frac{k_2}{m_1} \cdot x_2 + \frac{c_2 + c_1}{m_1} \cdot \dot{x}_1 - \frac{c_2}{m_1} \cdot \dot{x}_2 = \frac{k_1}{m_1} \cdot x_0 + \frac{c_1}{m_1} \cdot \dot{x}_0, \tag{6a}$$

$$\ddot{x}_i + \frac{k_i + k_{i+1}}{m_i} \cdot x_i - \frac{k_{i+1}}{m_i} \cdot x_{i+1} - \frac{k_i}{m_i} \cdot x_{i-1} + \frac{c_{i+1} + c_1}{m_i} \cdot \dot{x}_i - \frac{c_{i+1}}{m_i} \cdot \dot{x}_{i+1} - \frac{c_i}{m_i} \cdot \dot{x}_{i-1} = 0 \quad (i = 2, \ldots, 5), \tag{6b}$$

$$\ddot{x}_6 + \frac{k_6}{m_6} \cdot x_6 - \frac{k_6}{m_6} \cdot x_5 + \frac{c_6}{m_6} \cdot \dot{x}_6 - \frac{c_6}{m_6} \cdot \dot{x}_5 = 0. \tag{6c}$$

In order to express the equations of motion as functions of the ground displacement (x_0) alone, the following set of corresponding auxiliary equations is introduced:

$$\ddot{\psi}_1 + \frac{k_1 + k_2}{m_1} \cdot \psi_1 - \frac{k_2}{m_1} \cdot \psi_2 + \frac{c_2 + c_1}{m_1} \cdot \dot{\psi}_1 - \frac{c_2}{m_1} \cdot \dot{\psi}_2 = x_0, \tag{7a}$$

$$\ddot{\psi}_i + \frac{k_i + k_{i+1}}{m_i} \cdot \psi_i - \frac{k_{i+1}}{m_i} \cdot \psi_{i+1} - \frac{k_i}{m_i} \cdot \psi_{i-1} + \frac{c_{i+1} + c_i}{m_i} \cdot \dot{\psi}_i - \frac{c_{i+1}}{m_i} \cdot \dot{\psi}_{i+1} - \frac{c_i}{m_i} \cdot \dot{\psi}_{i-1} = 0 \quad (i = 2, \ldots, 5), \tag{7b}$$

$$\ddot{\psi}_6 + \frac{k_6}{m_6} \cdot \psi_6 - \frac{k_6}{m_6} \cdot \psi_5 + \frac{c_6}{m_6} \cdot \dot{\psi}_6 - \frac{c_6}{m_6} \cdot \dot{\psi}_5 = 0. \tag{7c}$$

Notice that the left-hand side of the above equations are of the same form as those of their counterparts [Eq. (6)]. The difference is in the right-hand side of Eq. (7a), where only the ground motion displacement is used as excitation (not its derivative). The ψ_i's may be thus interpreted as the fictitious transversal displacements corresponding to the x_i's of the original equations of motion under this modified excitation. This procedure is followed in order to define the simulation model's *state variables* as (for $i = 1, 2, \ldots, 6$):

$$z_i = \psi_{(i+1)/2} \quad (i \,\text{odd}), \quad z_i = \dot{\psi}_{i/2} \quad (i \,\text{even}). \tag{8}$$

Now, applying the principle of superposition [in doing so one has to compare, again, the right-hand side of Eqs. (6a) and (7a)], the actual storey displacements and accelerations are given by the following linear transformations of the auxiliary variables (the fictitious displacements) and their derivatives (the interested

reader is referred to the appendix for derivation details):

$$x_i = \frac{k_1}{m_1}\cdot\psi_i + \frac{c}{m_1}\cdot\dot{\psi}_i, \quad \ddot{x}_i = \frac{k_1}{m_1}\cdot\ddot{\psi}_i + \frac{c}{m_1}\cdot\dddot{\psi}_i \quad (i = 1, 2, \ldots, 6). \tag{9}$$

Note that the $\dddot{\psi}_i$'s appearing in the second set of equations above may be obtained for every storey (except for the first) through differentiation of Eqs. (7b), (7c). Finally, using Eqs. (7) and (9) under the definitions of Eq. (8), the equations relating the ground displacement to the 6th storey acceleration may be written into the *state-space form* as follows:

$$\dot{\mathbf{z}} = \mathbf{A}\mathbf{z} + \mathbf{b}x_0, \tag{10a}$$

$$\ddot{x}_6 = \mathbf{c}^{\mathrm{T}}\mathbf{z} \tag{10b}$$

with $\mathbf{A}$, $\mathbf{b}$, $\mathbf{c}$ designating proper matrix/vector quantities and $\mathbf{z} \triangleq [z_1\ z_2\ \ldots z_6]^{\mathrm{T}}$.

2.2. Damage cases

The damage cases considered correspond to reductions in the stiffness characteristics of the building storeys in the simulation model. Therefore six *fault modes* (each fault mode comprising the continuum of damage of all possible magnitudes incurred in a particular storey; also see Section 3.4), are considered (note that the terms fault and damage are presently treated as interchangeable). Monte Carlo experiments, in each one of which 0% (no damage), 5%, or 20% damage is introduced as reduction in the stiffness characteristics of each storey, are performed (20 simulation runs per case). These faults are designated as F_0^i, $F_{0.05}^i$, or $F_{0.20}^i$, respectively, with the superscript i indicating the storey of damage occurrence, and the subscript the damage level (stiffness reduction).

It is, at this point, interesting to examine the sensitivity of the theoretical frequency response function (frf) of the building simulation model (transfer function $\ddot{X}_6/X_0$) with respect to the considered damage cases. Fig. 2 depicts the theoretical Bode (frf) diagram for the nominal (healthy) structure (frequency range 0–10 Hz; see Section 2.3), as well as for the structure in the presence of damage incurred in the third storey at both the 5%

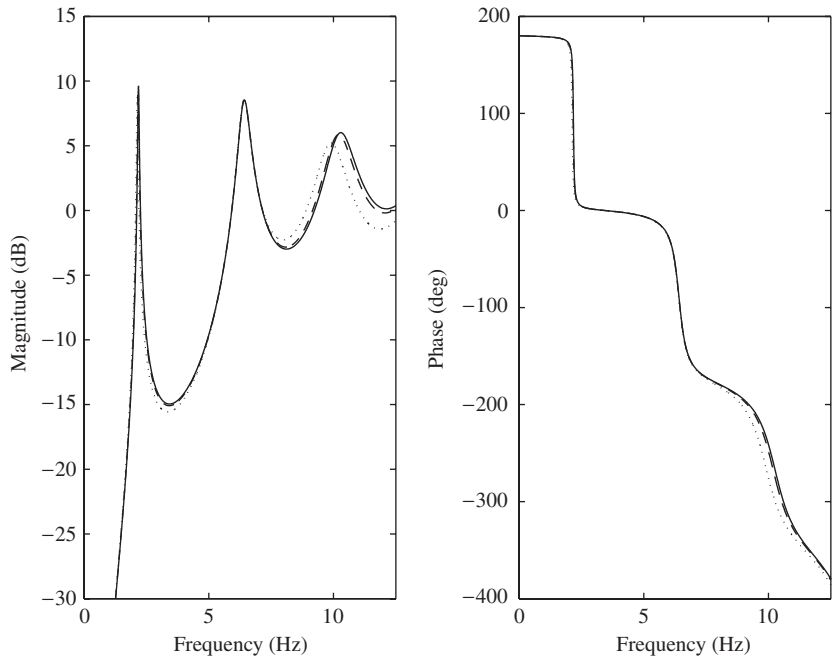

Fig. 2. Sensitivity of the structural dynamics (simulation model) with respect to damage: theoretical Bode diagram of the nominal structure (—), the structure under an $F_{0.05}^3$ fault (- - -), and the structure under an $F_{0.20}^3$ fault (...) [$\ddot{X}_6/X_0$ transfer function].

Table 2
Effects of damage (5% and 20% stiffness reduction in the 3rd storey) on the simulation model's first three natural frequencies

Natural frequency (Hz)	Healthy structure	5% damage ($F^3_{0.05}$)	20% damage ($F^3_{0.20}$)
f_{n1}	2.18	2.17	2.12
f_{n2}	6.41	6.41	6.40
f_{n3}	10.28	10.20	9.91

and 20% levels. The effects of the first (5%) damage are essentially negligible in the diagram, while those of the second (20%) are more pronounced (reduction in the third modal frequency). The differences in the simulation model's first three natural frequencies induced by the two damage levels are presented in Table 2 as well (frequency range 0–10 Hz). It should be nevertheless noted that the present damage detection and assessment methodology utilizes the parameters of the identified OE model (see Section 3); these are functions of *all* modal parameters, not just the natural frequencies.

2.3. Seismic excitation and model simulation

The prototype seismic ground displacement signal used in the study is obtained through integration (via a specific procedure [40,41]) of an earthquake ground acceleration signal recorded during a 1993 event in Patras, Greece (sampling frequency $f_s = 200$ Hz; signal duration 37.04 s or 7408 samples; "strong" excitation duration of 6.52 s; maximum recorded acceleration $0.109g$).

The prototype displacement signal is modelled via the recursive autoregressive moving average (RARMA)—recursive maximum likelihood (RML) adaptive filtering type approach [35]. This leads to a RARMA representation of orders 3 and 8 [RARMA(3,8) representation], with forgetting factor $\lambda = 0.975$ and non-parametrically estimated innovations variance (sliding window with $K_1 = 2$, $K_2 = 4$, $\lambda_1 = \lambda_2 = 0.95$; for details on the approach used the interested reader is referred to Ref. [35]). Artificial earthquake ground displacement signals for the Monte Carlo experiments are then generated by driving the obtained RARMA(3,8) representation via innovations characterized by the estimated non-stationary variance.

As the energy content of the prototype and generated signals is limited to the 0–10 Hz frequency range, at most the first three of the building's modes (see Table 1) may be excited. As a consequence, structural damage detection and assessment have to be based upon *partial* information in both the *spatial* (only one response, that of the 6th storey) and the *frequency bandwidth* (low-frequency content) senses.

The generated excitation (ground displacement) and resulting building response (6th storey acceleration) are, in each case, low-pass filtered (via a 16th order Chebyshev II filter with cut-off at $f_c = 10$ Hz) and re-sampled at $f_s = 25$ Hz. Each response acceleration signal is then corrupted by non-stationary uncorrelated noise at the 5% noise-to-signal (N/S) local level (in the standard deviation sense). The constant sample means are finally subtracted from the ground excitation and noise-corrupted building response signals (each being $N = 926$ samples long).

Typical constant sample mean-corrected ground excitation and noise-corrupted building (simulation model) response (6th storey acceleration) signals are, along with non-parametric estimates of their time-dependent power spectral densities (PSDs; Welch method employing a 128 sample long moving window; Hanning data windowing [42]), depicted in Fig. 3. The *non-stationarity* of both signals is evident in terms of variance and frequency (spectral) content. Furthermore, the acceleration response reveals higher-energy concentration in the vicinities of 2, 6 and 9 Hz; evidently, this is in gross agreement with the structure's modal frequencies.

3. The stochastic OE model-based damage detection and assessment methodology

3.1. Principles

As previously indicated, the stochastic OE model-based damage detection and assessment methodology is intended for *periodically* assessing the state of a structure, *following* potential damage occurrence. It is to be

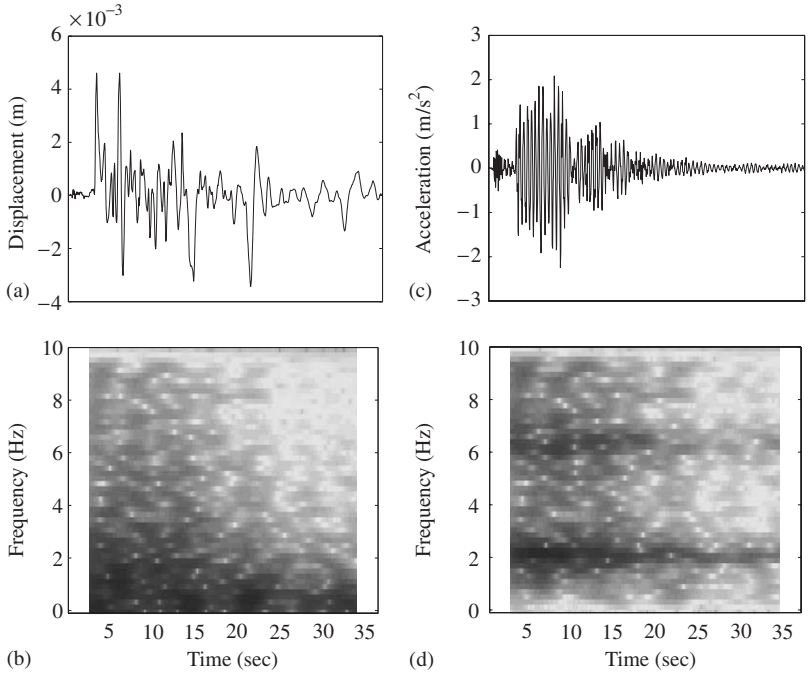

Fig. 3. Typical excitation (ground displacement) and structural response (6th storey acceleration) signals for the nominal structure: (a) excitation, (b) excitation's time-dependent PSD estimate, (c) response, (d) response's time-dependent PSD estimate (darker areas designate higher spectral magnitude).

used with *low-level* earthquake excitations under which the structure operates within its *linear* regime. The methodology assesses changes in the dynamics, as expressed in the identified model relating two (or more) locations on which vibration measurements are taken.

The methodology is based upon:

(a) Stochastic OE identification of a "small" size (few estimated parameters) *simple* and *partial* structural model in *parametric* form. This *OE model* is identified from measured excitation–response signals (presently the ground displacement and the 6th storey acceleration), without any knowledge of the "larger" size simulation model of Section 2.1. The identified OE model is thus solely based upon the measured signals and attempts to provide a *partial* representation of the structure in the:
- *Spatial* sense (only the ground excitation and the 6th storey response are measured),
- *Frequency bandwidth* sense (only the low-frequency range is used).

The *interval estimate* (point estimate and covariance) of the OE model parameter vector forms the "raw" feature vector utilized by the damage detection and assessment procedures.

(b) Statistical hypothesis testing for effective damage detection under uncertainty.

(c) A GM [16,38] for damage assessment, that is for damage gross localization and quantification.

3.2. Stochastic OE model identification

OE model identification aims at the estimation of a discrete-time structural model of the OE form. In the simplest case of single excitation single response (two measured signals) this is

$$y[t] = \frac{B(\mathscr{B})}{A(\mathscr{B})} \cdot x[t] + e[t] \tag{11}$$

relating the sampled versions of the excitation $x[t]$ and response $y[t]$ signals (within the context of the present paradigm the ground displacement $x_0[t]$ and the noise-corrupted 6th storey acceleration signals $\ddot{x}_6[t]$, respectively; see Refs. [37,43] on the justification of using OE and related models for structural dynamics identification). In this expression t designates normalized discrete time ($t = 0, 1, 2, \ldots$, with the corresponding absolute time being $t \cdot T_s$ and T_s standing for the sampling period) and $e[t]$ a zero-mean model residual error (or OE) representing the non-stationary noise corrupting the response. $A(\mathscr{B})$, $B(\mathscr{B})$ are polynomials in the backshift operator ($\mathscr{B} \cdot x[t] \triangleq x[t-1]$) of the following respective forms:

$$A(\mathscr{B}) \triangleq 1 + a_1 \cdot \mathscr{B} + \cdots + a_{n_a} \cdot \mathscr{B}^{n_a}, \quad B(\mathscr{B}) \triangleq b_0 + b_1 \cdot \mathscr{B} + \cdots + b_{n_b} \cdot \mathscr{B}^{n_b}. \tag{12}$$

Notice that $A(\mathscr{B})$, $B(\mathscr{B})$ are referred to as the autoregressive (AR) and exogenous (X) polynomials, respectively. Their degrees, n_a and n_b, are referred to as the AR and X orders, while their parameters, a_i and b_i, are referred to as the AR and X parameters.

A model of the form of Eq. (11) is referred to as an OE model of orders (n_a, n_b) [in short OE(n_a, n_b) model] [36, pp. 85–86; 37]. In the time domain it may be expressed as

$$y[t] + \sum_{i=1}^{n_a} a_i \cdot y[t-i] = \sum_{i=0}^{n_b} b_i \cdot x[t-i] + e[t] + \sum_{i=1}^{n_a} a_i \cdot e[t-i]. \tag{13}$$

A main advantage of the OE model is that it is capable of accounting for noise effects without resorting on an explicit noise representation, thus overcoming some of the difficulties associated with noise non-stationarity. Model estimation may be based upon minimization of a quadratic functional of the OE, that is:

$$\hat{\boldsymbol{\theta}} \triangleq \arg\min_{\boldsymbol{\theta}} J(\boldsymbol{\theta}) \triangleq \arg\min_{\boldsymbol{\theta}} \frac{1}{N} \sum_{t=0}^{N-1} e^2[t], \tag{14}$$

where argmin stands for "argument minimizing", the hat designates estimator/estimate, N the signal length (in samples), and $\boldsymbol{\theta}$ the model parameter vector consisting of the AR and X parameters:

$$\boldsymbol{\theta} \triangleq [a_1\, a_2 \ldots a_{n_a} \vdots\, b_0\, b_1\, b_2 \ldots b_{n_b}]^{\mathrm{T}}. \tag{15}$$

Minimization of the $J(\boldsymbol{\theta})$ criterion is achieved via nonlinear optimization based upon the Levenberg–Marquardt scheme [36, p. 328]. Under mild conditions, the estimator is asymptotically ($N \to \infty$) Gaussian distributed with mean equal to the true parameter vector $\boldsymbol{\theta}^o$ and covariance matrix $\mathbf{P}$ [36, pp. 240–242], that is:

$$\hat{\boldsymbol{\theta}} \sim \mathscr{N}(\boldsymbol{\theta}^o, \mathbf{P}) \tag{16}$$

with $\mathscr{N}(\cdot, \cdot)$ designating Gaussian (normal) distribution with the indicated mean and covariance.

Model order selection is based upon the successive estimation of increasingly higher-order models and examination of the achieved OE $J(\hat{\boldsymbol{\theta}})$, as well as model *dispersion analysis* (DA). The OE functional, although generally decreasing with increasing model order, is expected to reach a "plateau" as soon as the adequate model order is reached. The DA [37,43], on the other hand, provides the fraction of the vibration signal energy associated with each estimated mode, and is indirectly used for model order determination, as unnecessary ("extraneous") modes (and thus unnecessarily high-order models) may be detected by their small dispersions. Once an adequate model has been selected, complete modal information, in terms of natural frequencies, damping ratios, modal residues, and modal dispersions, may be readily obtained [37,43].

3.3. Damage detection

Damage detection is based upon the comparison of the OE model parameter vector [Eq. (15)] (or a selected part of it) for the identified *nominal* (healthy) structural model with that of the identified *current* structural model (the structure being in an unknown state). The former is obtained in an initial (off-line) *training stage*, while the latter is obtained during the *testing (operational) stage*. Notice that this approach is different from residual-based methods in which no identification is performed in the testing stage.

Let $\hat{\boldsymbol{\theta}}^h$ and $\hat{\boldsymbol{\theta}}^u$ designate the parameter vectors corresponding to the healthy and current (unknown) states of the structure, respectively. Due to the estimator consistency and Gaussianity:

$$\hat{\boldsymbol{\theta}}^h \sim \mathcal{N}(\boldsymbol{\theta}^{ho}, \mathbf{P}^h) \quad \text{and} \quad \hat{\boldsymbol{\theta}}^u \sim \mathcal{N}(\boldsymbol{\theta}^{uo}, \mathbf{P}^u) \tag{17}$$

with $\boldsymbol{\theta}^{ho}$, $\boldsymbol{\theta}^{uo}$ designating the respective true vectors and $\mathbf{P}^h$, $\mathbf{P}^u$ the corresponding covariance matrices. The vectors' Gaussianity, coupled with their mutual independence, implies that their difference follows Gaussian distribution as well, that is

$$\delta\hat{\boldsymbol{\theta}} = \hat{\boldsymbol{\theta}}^h - \hat{\boldsymbol{\theta}}^u \sim \mathcal{N}(\delta\boldsymbol{\theta}^o, \delta\mathbf{P}) \tag{18}$$

with $\delta\boldsymbol{\theta}^o$ designating the true difference vector and $\delta\mathbf{P} = \mathbf{P}^h + \mathbf{P}^u$ the corresponding covariance matrix.

Damage detection may be then based upon examination for changes in the parameter vector via the hypothesis testing problem:

$$\mathrm{H}_0 : \delta\boldsymbol{\theta}^o = \mathbf{0} \quad \text{(Healthy structure)},$$

$$\mathrm{H}_1 : \delta\boldsymbol{\theta}^o \neq \mathbf{0} \quad \text{(Damaged structure)}.$$

Indeed, under the null (H_0) hypothesis $\delta\hat{\boldsymbol{\theta}} \sim \mathcal{N}(0, \delta\mathbf{P} = 2\mathbf{P}^h)$ and the following S statistic follows χ^2 distribution with $d = n_a + n_b + 1$ (parameter vector dimensionality) degrees of freedom (as it may be shown to be the sum of squares of independent, standardized, Gaussian random variables [44]), that is

$$S = \delta\hat{\boldsymbol{\theta}}^{\mathrm{T}} \delta\mathbf{P}^{-1} \delta\hat{\boldsymbol{\theta}} \sim \chi^2(d). \tag{19}$$

Since the covariance $\mathbf{P}^h$ corresponding to the healthy structure is unavailable, its sample (estimated) version $\hat{\mathbf{P}}^h$ is used in practice. Treating this sample covariance as a deterministic quantity, that is a quantity characterized by negligible variability (which is reasonable for large N), leads to the following multivariate test at the α risk level (probability of type I error, that is rejecting H_0 although it is correct, equal to α):

$$\begin{aligned} S < \chi^2_{1-\alpha}(d) \quad &\Longrightarrow \quad \mathrm{H}_0 \quad \text{is accepted} \\ &\qquad\quad \text{(no damage is detected)} \\ \text{Else} \quad &\Longrightarrow \quad \mathrm{H}_0 \quad \text{is rejected} \\ &\qquad\quad \text{(damage is detected)} \end{aligned}$$

with $\chi^2_{1-\alpha}(d)$ designating the χ^2 distribution's $1-\alpha$ critical point.

Alternatively (although suboptimally), individual statistical tests on the parameter vector's components could be considered. Indeed, under the null (H_0) hypothesis, the ith component of $\delta\hat{\boldsymbol{\theta}}$, designated as $\delta\hat{\theta}_i$, follows Gaussian distribution:

$$\delta\hat{\theta}_i \sim \mathcal{N}(\delta\theta_i^o, \delta P_{i,i}).$$

Replacing the unknown variance $\delta P_{i,i}$ with its sample (estimated) version $\delta\hat{P}_{i,i}$ leads to a t-distributed $\delta\hat{\theta}_i / \sqrt{\delta\hat{P}_{i,i}}$ random variable (ratio of a Gaussian over a χ^2 random variable [44]) with $N - n_a - n_b - 2$ degrees of freedom (n_a, n_b, and N designating the AR order, X order, and the signal length in samples, respectively). This leads to the following univariate test for damage detection at the α risk level:

$$\begin{aligned} t_{\alpha/2}\sqrt{\delta\hat{P}_{i,i}} \leqslant \delta\hat{\theta}_i \leqslant t_{1-\alpha/2}\sqrt{\delta\hat{P}_{i,i}} \quad \forall i \quad &\Longrightarrow \quad \mathrm{H}_0 \quad \text{is accepted} \\ &\qquad\quad \text{(no damage is detected)} \\ \text{Else} \quad &\Longrightarrow \quad \mathrm{H}_0 \quad \text{is rejected} \\ &\qquad\quad \text{(damage is detected)} \end{aligned}$$

with t_α designating the t distribution's α critical point.

3.4. Damage assessment

As already indicated, damage assessment includes both gross localization and quantification. Like damage detection, it is based upon the identified OE model parameter vector.

3.4.1. Damage localization

Once damage has been detected, localization (also referred to as damage identification) is accomplished via a *GM* originally developed in a broader context by the second author and his co-worker [16,38].

Toward this end, in the initial *training stage* the model parameter vector $\boldsymbol{\theta}$ (or a selected part of it) of the OE model is used as an initial feature vector, which is subsequently linearly transformed via the Karhunen–Loeve expansion (principal component analysis) [38; 45, p. 66] into a coordinate system in which information compression (feature vector reduction) may be best achieved. Feature vector dimensionality reduction (to dimensionality M) is then achieved by selecting the loss of information (expressed in terms of logarithmic entropy) that is to be allowed. Following this selection, a *stochastic feature space* is defined as the space spanned by the $2M$-dimensional vector $\boldsymbol{\theta}_K$ consisting of the mean values and variances of the elements of the transformed and reduced feature vector.

A key idea in damage localization is the notion of fault mode and its geometric representation within the defined stochastic feature space. *Fault mode* refers to the multitude of faults (damages), of all possible levels, characterized by a common, specific, cause. For instance, in this study's paradigm, a fault mode consists of all possible levels of stiffness reduction in a particular storey. Evidently, an infinite number of damage levels is included in each fault mode. Damage localization (identification) then refers to the identification of the particular fault mode to which a detected damage belongs.

For exploiting this idea, a number of experiments in which p different levels of damage are, for each one of the specified N_F fault modes, injected into the simulation model (in general a finite-element model, or, possibly, a laboratory scale model could be used) are performed (*training stage*). From each such experiment an interval estimate of $\boldsymbol{\theta}$ is obtained, and a corresponding (transformed and reduced to dimensionality M) feature vector estimate is computed. This leads to p estimates of $\boldsymbol{\theta}_K$ per fault mode, which are used for the construction of a geometric representation of each fault mode in the form of a $(2M-1)$-dimensional hyperplane. The ith fault mode hyperplane is represented as

$$g^i(\boldsymbol{\theta}_K) = \theta_{K_1} + \omega_1^i \cdot \theta_{K_2} + \cdots + \omega_{2M-1}^i \cdot \theta_{K_{2M}} - \omega_{2M}^i = 0 \tag{20}$$

with θ_{K_j} indicating the jth element of $\boldsymbol{\theta}_K$ and ω_j^i the hyperplane's jth coefficient, which is estimated via linear regression [38].

Once damage is detected (during the *testing stage*), the transformed and reduced feature vector $\boldsymbol{\theta}_K^u$ corresponding to the current state of the structure is obtained. Fault mode identification (damage localization) is then achieved by computing the distances between the feature vector's tip point and each fault mode hyperplane. The structure is then identified as being in that fault mode with the hyperplane of which the distance is minimal, that is

$$i^\star = \text{index} \min_{i\in[1,N_F]} \left\{ \min_{\boldsymbol{\theta}_K \in G^i} D(\boldsymbol{\theta}_K, \boldsymbol{\theta}_K^u) \right\} \tag{21}$$

with $D(\cdot,\cdot)$ designating Euclidean (or other proper distance), $G^i \triangleq \{\boldsymbol{\theta}_K | g^i(\boldsymbol{\theta}_K) = 0\}$, and $i = 1, 2, \ldots, N_F$. The reader is referred to Sadeghi and Fassois [16,38] for details.

3.4.2. Damage quantification (level estimation)

The approach presently introduced for damage quantification is based upon evaluation of the distance between the tip of $\boldsymbol{\theta}_K^u$ and the point corresponding to the nominal (healthy) structure. Distances should have been properly pre-calibrated in the training stage in order to accurately reflect damage level.

4. Damage detection and assessment results

As already stated, damage detection and assessment is presently based upon a single pair of vibration measurements, that of the ground displacement x_0 and the 6th storey acceleration $\ddot{x}_6$. Moreover, due to the nature of the excitation, only the 0–10 Hz frequency range is employed.

4.1. Training stage

4.1.1. OE identification of the nominal (healthy) structure

For the OE identification of the nominal (healthy) structure, a sequence of OE(n_a, n_b) models with $n_a, n_b \in [6, 12]$ is fitted to the corresponding $N = 926$ sample long ground excitation and noise-corrupted response signals. The estimated OE(6,6) model ($b_0 \neq 0$) is found to be adequate in terms of achieved OE and simulation capability, and is also verified as such through DA [43]. This selection also is in obvious agreement with the presence of three modes in the building's simulation model of Section 2.1 within the excitation frequency range (Table 1). A typical 6th storey response signal, along with its OE(6,6) model-based reconstruction (simulation) and the corresponding output error, are presented in Fig. 4, from which the excellent performance of the selected OE(6,6) model is confirmed.

Monte Carlo experiments, in which OE(6,6) models are fitted to pairs of excitation and noise-corrupted response signals obtained from the nominal structure (simulation model), are subsequently conducted. Identification results from these experiments are, in the form of estimated modal parameters for the modes of interest (first three modes), presented in Table 3. Evidently, the agreement between the obtained estimates and their theoretical counterparts is very good, and the attained standard deviations quite small. This applies to mode 3 as well, even though it is in fact located slightly beyond the 10 Hz cut-off frequency (in the range close to 10 Hz even the original excitation is relatively weak; see Fig. 3). The Bode (frf) diagrams of the estimated models are also compared to their theoretical (simulation model) counterpart in Fig. 5, from which excellent agreement is observed for both the spectral peaks and valleys. It is also worth observing that the variability of the estimates is particularly low within the excitation frequency range of 0–10 Hz.

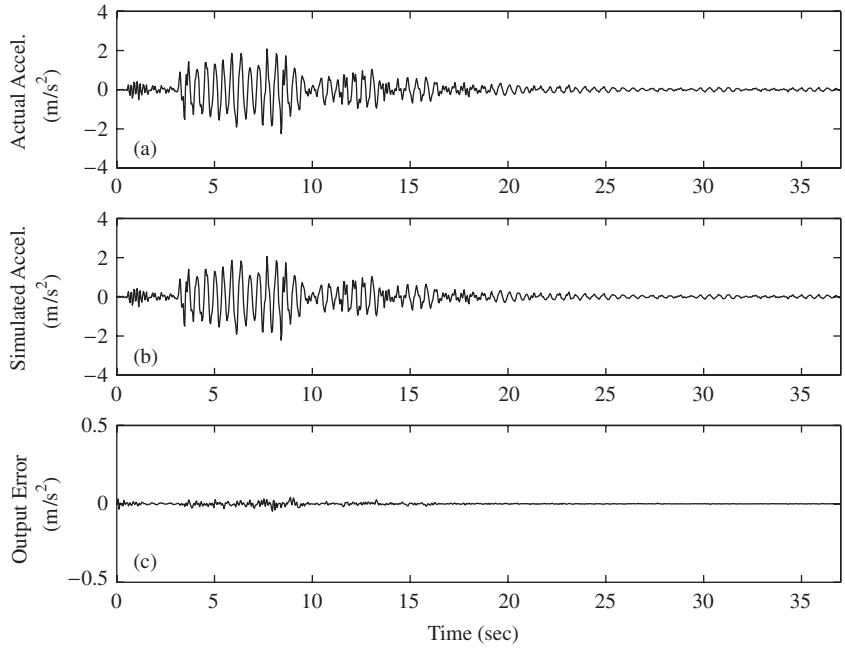

Fig. 4. Typical OE identification of the nominal structure: (a) 6th storey actual acceleration, (b) its OE(6,6) model-based counterpart, (c) the corresponding output error.

Table 3
OE-based identification of the modal characteristics of the seismically excited nominal structure [discrete $\ddot{X}_6/X_0$ transfer function; 20 Monte Carlo runs; OE(6,6) model]

Mode	Natural frequency[a] (Hz)	Damping ratio[a] (%)
1	$2.18\ (2.18 \pm 3.12 \times 10^{-5})$	$1.21\ (1.21 \pm 1.71 \times 10^{-3})$
2	$6.41\ (6.41 \pm 1.55 \times 10^{-3})$	$3.56\ (3.56 \pm 1.56 \times 10^{-2})$
3	$10.28\ (10.26 \pm 4.37 \times 10^{-2})$	$5.70\ (4.60 \pm 2.39 \times 10^{-1})$
Mode	**Dispersion[a] (%)**	**Residue[a]**
1	$6.03\ (5.91 \pm 0.23)$	1.0, j0.0 (1.0, j0.0)
2	$39.91\ (39.12 \pm 1.62)$	7.689, j0.306 (7.538 ± 0.022, j1.457 ± 0.044)
3	$54.06\ (54.97 \pm 1.85)$	15.349, −j0.577 (13.532 ± 0.675, −j0.704 ± 0.095)

[a]True (estimated ± standard deviation).

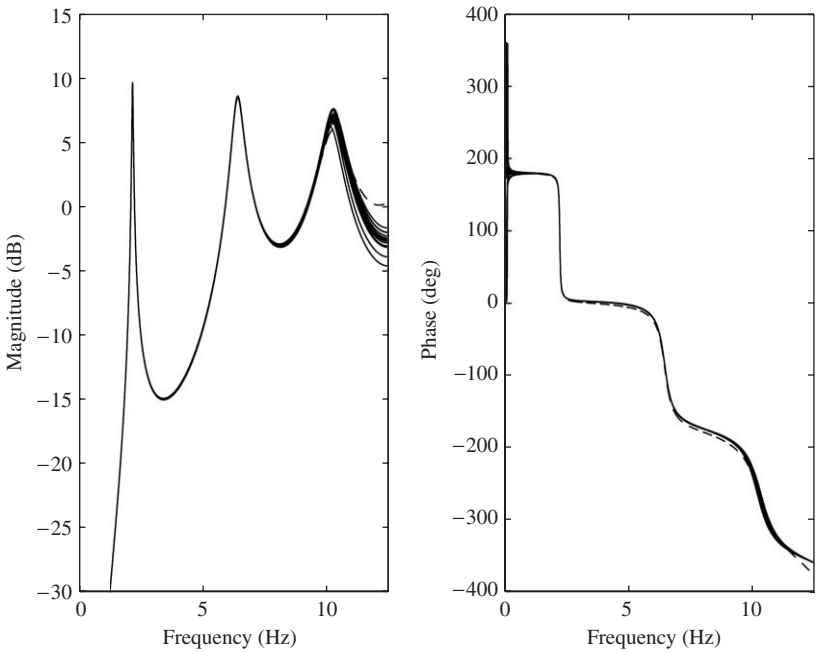

Fig. 5. OE identification accuracy: Bode diagrams of estimated OE(6,6) models (—) and the theoretical structure (simulation model;- - -) [$\ddot{X}_6/X_0$ transfer function; 20 Monte Carlo runs; nominal structure].

4.1.2. Feature vector selection and fault mode representation

For damage localization the initial (“raw”) feature vector consists of the OE model parameters ($n = n_a + n_b + 1 = 13$ parameters) and coincides with the vector used for damage detection. This is subsequently linearly transformed. The normalized entropy of several transformed feature vectors corresponding to the nominal structure is computed, and preservation of 97% of the entropy leads to a dimensionality of $M = 3$ (Fig. 6) for the transformed and reduced (truncated) feature vector. The $\boldsymbol{\theta}_K$ vector is thus six-dimensional, consisting of the means and variances of the reduced feature vector elements. Following this, the six fault mode hyperplanes ($F^1 \ldots F^6$), each corresponding to damage incurred in the stiffness characteristics of each storey, are constructed based upon signals obtained by injecting damage of various levels ($1 \ldots 30\%$) in the simulation model.

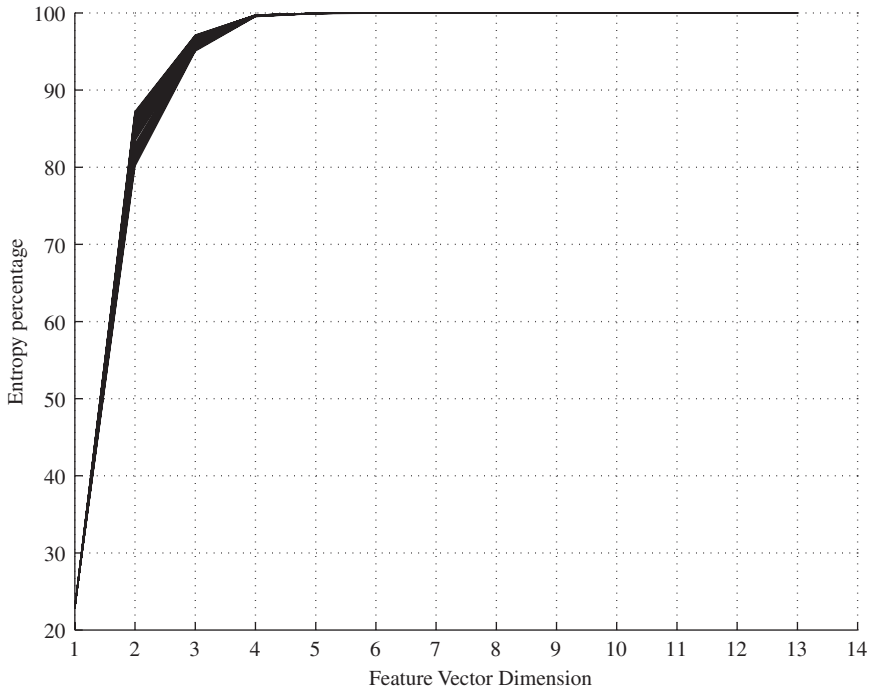

Fig. 6. Normalized logarithmic entropy of the transformed feature vectors versus feature vector dimensionality (nominal structure; 20 Monte Carlo runs).

4.2. Testing (operational) stage

4.2.1. Damage detection

Damage detection is based upon the current OE model parameter vector. Typical results, obtained via the multivariate test for the $F^3_{0.05}$ and $F^3_{0.20}$ damage cases (5% and 20%, respectively, reduction in the 3rd storey stiffness characteristics; 20 Monte Carlo runs per fault case) are presented in Fig. 7. Evidently, all damage cases are clearly detected as such, as the S statistic always exceeds the critical point $\chi^2_{0.95}(13) = 22.36$ at the selected $\alpha = 0.05$ risk level. Similar results are obtained via univariate tests, with each one applied on each scalar parameter. Two indicative such results are, for an $F^3_{0.05}$ damage case and an $F^3_{0.20}$ damage case, presented in Fig. 8, from which detection is clearly achieved based upon the a_1 and a_3 parameter tests ($F^3_{0.05}$ damage) and the $a_1, \ldots, a_5$ parameter tests ($F^3_{0.20}$ damage). Similar results are obtained for damage incurred in other storeys of the building.

4.2.2. Damage assessment

Damage localization (*identification*): Two typical damage localization (identification) results, the first corresponding to an $F^3_{0.05}$ damage case and the second to an $F^3_{0.20}$ damage case, are presented in Fig. 9. In these plots the distances of the current (building in unknown state) $\boldsymbol{\theta}^u_K$ vector's tip point to each fault mode hyperplane are depicted. As is readily verified, the distance to the correct (F^3) hyperplane is, in both cases, clearly minimal, and thus the methodology correctly identifies each damage as incurred in the building's third storey.

Damage quantification (*level estimation*): For damage quantification a distance versus fault magnitude function is, for each fault mode, employed. This is pre-constructed during the training stage, by taking damage cases from a specific fault mode but of various (known) levels and computing their distance from the point corresponding to the nominal (healthy) structure. The distance function for the F^3 (3rd storey) mode is depicted in Fig. 10. Using this function for damage level estimation with the two single damage cases ($F^3_{0.05}$ and $F^3_{0.20}$) leads to very accurate estimates (5% and 20%, respectively; see Fig. 10).

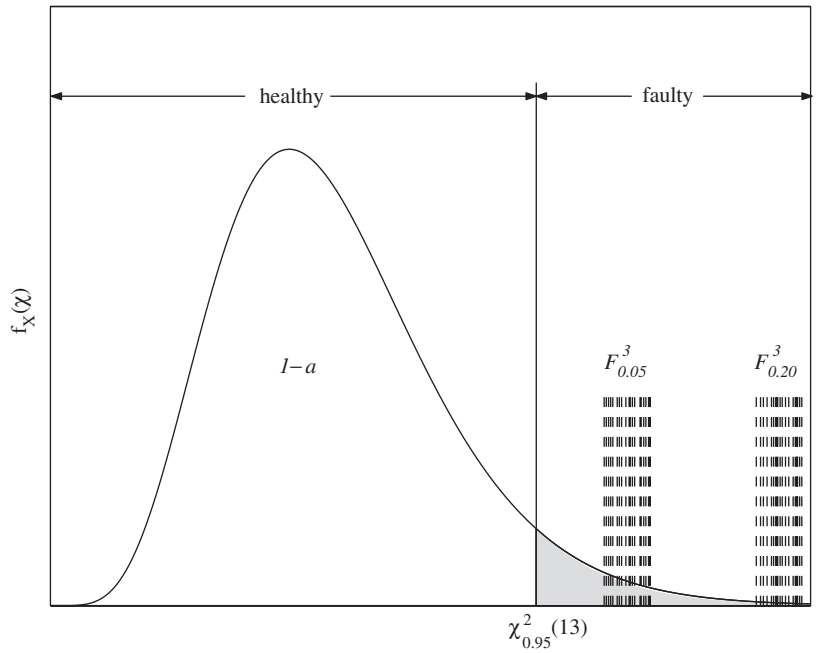

Fig. 7. Monte Carlo structural damage detection results based upon the multivariate test ($F^3_{0.05}$ and $F^3_{0.20}$ fault cases; 20 runs per case; risk level $\alpha = 0.05$).

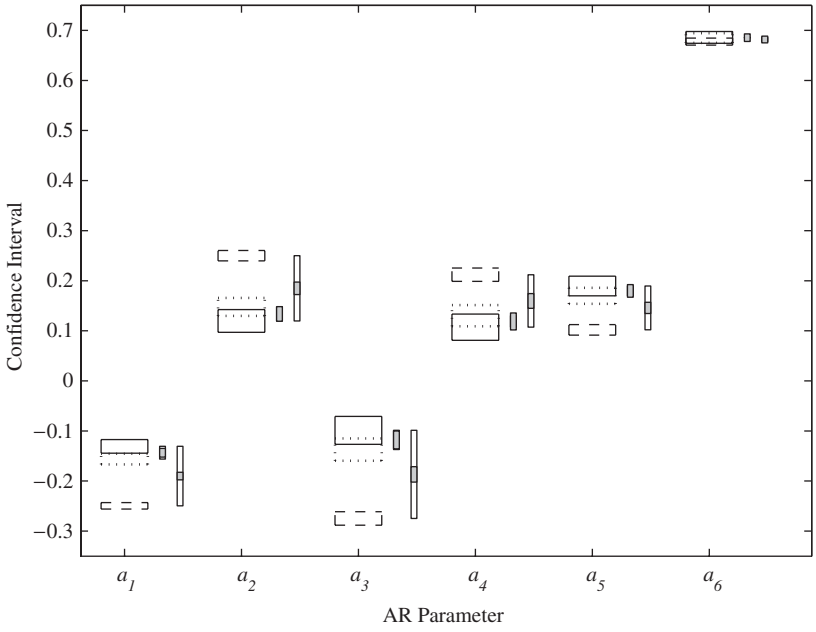

Fig. 8. Structural damage detection results based upon univariate tests: $F^3_{0.05}$ (...) and $F^3_{0.20}$ (---) fault cases compared to the nominal structure (—). The wide bars designate parameter confidence intervals at the $\alpha = 0.05$ level. The narrow bars designate $|\delta\hat{\theta}_i|$ (white) and $1.96\sqrt{\hat{P}_{ii}}$ (gray). A fault is detected if a white bar contains the corresponding gray.

5. Concluding remarks and discussion

A stochastic OE model-based methodology for damage detection and assessment in structures under earthquake excitation has been introduced. The methodology is intended for periodically assessing the state of

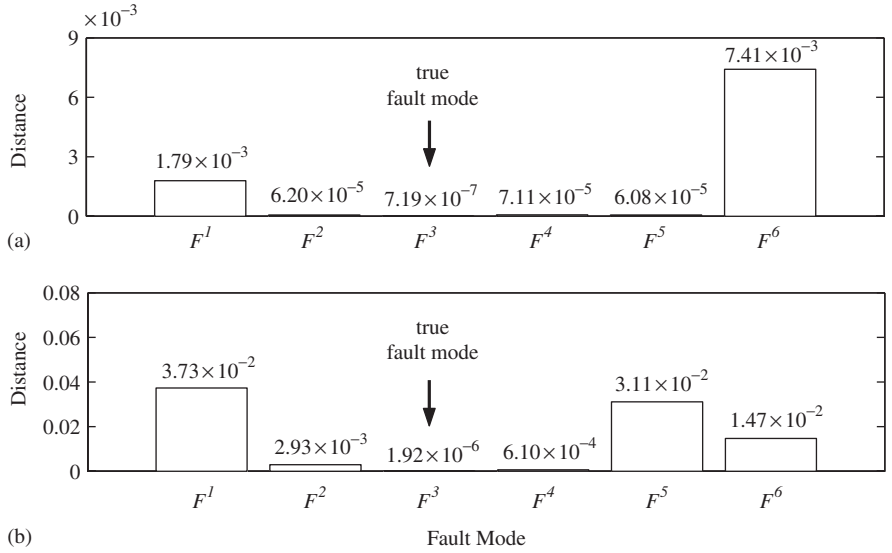

Fig. 9. Structural damage localization results for an $F^3_{0.05}$ (a) and an $F^3_{0.20}$ (b) damage case: distances of the current fault point to each hyperplane (the fault mode corresponding to minimal distance is identified; see Section 3.4.1).

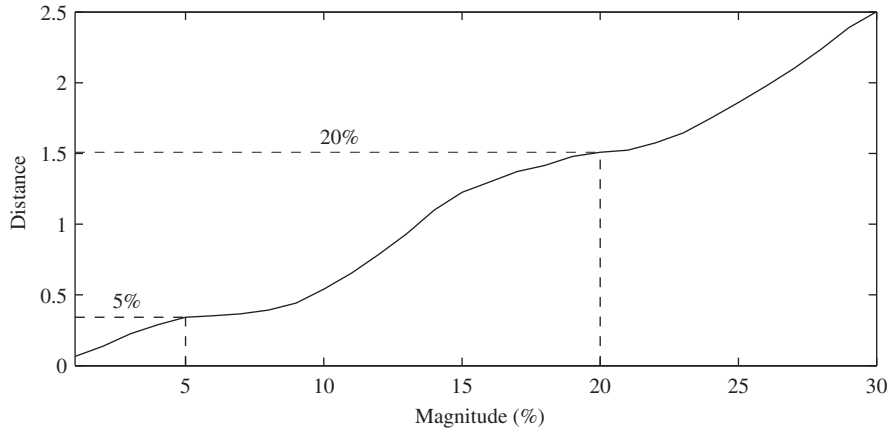

Fig. 10. Structural damage quantification results for an $F^3_{0.05}$ and an $F^3_{0.20}$ damage case: distance function (see Section 3.4.1) versus fault magnitude (level) for the F^3 fault mode.

a structure following potential damage occurrence by exploiting vibration measurements produced by low-level earthquake excitations. It is based upon stochastic OE model identification, statistical hypothesis testing procedures that utilize the properties of the OE estimator for effective damage detection, and a GM for damage assessment (localization and quantification).

The methodology circumvents the problems associated with earthquake excitation non-stationarity and limited duration, and is capable of operating under measurement uncertainty. It utilizes only "small" size, simple and partial (in both the spatial and frequency bandwidth senses) identified structural models, and a limited number of measured signals.

Its feasibility and effectiveness have been demonstrated via Monte Carlo experiments pertaining to damage detection and assessment in a simple simulation model of a six storey building subject to earthquake excitation. Damage detection, localization and quantification have been shown to be effective with damage

levels of 5% and 20% reduction in a storey's stiffness by using acceleration responses corrupted with 5% non-stationary noise.

Just like any vibration-based method, the methodology's performance (in particular the detectable level of damage) is in practice affected by a number of factors, such as: (i) The earthquake excitation characteristics (direction, strength, duration, and frequency content), which must be sufficient for successful identification. (ii) The number and specific selection of the vibration measurement locations. Although vibration methods are "global", it is well known that relatively minor damages are more effectively detected from certain measurement locations. (iii) Changes in the environmental effects between the training and operational stages (for instance changes in temperature and humidity), but also the presence of additional excitations due, for instance, to wind. This is a well known issue and is in the focus of a number of current investigations. (iv) The level of noise on the measured vibration signals. (v) Excursions from the structure's linear operating regime (which may be due to stronger earthquake events). (vi) Finally, damage assessment (localization and level estimation) accuracy depends upon the quality of the (finite element or other) model employed.

In addition, there are some limitations to the presented methodology. One such limitation is the gross nature of the achieved damage assessment, which is inherited from the simple and partial models used. Possibilities for more precise assessment could be considered in conjunction with expanded ("larger" size) structural models. Furthermore, although the method is fully capable of detecting multiple damage (damage at several locations), assessment is currently limited to the single damage case.

An additional, "internal", limiting factor is the approximate, linear (hyperplane-type) representations of the fault modes, which may (under certain conditions) lead to errors. Work has been under way for the relaxation of this limitation, and the precise estimation of nonlinear fault mode representations from pertinent vibration records. Progress on this, along with a detailed laboratory application, will be reported in a forthcoming paper [46].

Acknowledgments

The authors wish to thank two anonymous referees whose constructive comments led to improvements in the manuscript.

Appendix

Using the differentiation operator D ($Dx \triangleq \dot{x}$), the equations of motion [Eqs. (6)] are rewritten as

$$\underbrace{\left(D^2+\frac{c_{i+1}+c_i}{m_i}\cdot D+\frac{k_{i+1}+k_i}{m_i}\right)}_{A_i}\cdot x_i-\underbrace{\left(\frac{c_{i+1}}{m_i}\cdot D+\frac{k_{i+1}}{m_i}\right)}_{B_i}\cdot x_{i+1}=\underbrace{\left(\frac{c_i}{m_i}\cdot D+\frac{k_i}{m_i}\right)}_{C_i}\cdot x_{i-1}$$
$$(i=1,\ldots,5) \tag{A.1}$$

$$\underbrace{\left(D^2+\frac{c_6}{m_6}\cdot D+\frac{k_6}{m_6}\right)}_{G}\cdot x_6-\underbrace{\left(\frac{c_6}{m_6}\cdot D+\frac{k_6}{m_6}\right)}_{H}\cdot x_5=0. \tag{A.2}$$

The corresponding set of auxiliary equations [Eqs. (7)] is rewritten as:

$$\left(D^2+\frac{c_2+c_1}{m_1}\cdot D+\frac{k_2+k_1}{m_1}\right)\cdot\psi_1-\left(\frac{c_2}{m_1}\cdot D+\frac{k_2}{m_1}\right)\cdot\psi_2=x_0, \tag{A.3}$$

$$\left(D^2+\frac{c_{i+1}+c_i}{m_i}\cdot D+\frac{k_{i+1}+k_i}{m_i}\right)\cdot\psi_i-\left(\frac{c_{i+1}}{m_i}\cdot D+\frac{k_{i+1}}{m_i}\right)\cdot\psi_{i+1}=\left(\frac{c_i}{m_i}\cdot D+\frac{k_i}{m_i}\right)\cdot\psi_{i-1}$$
$$(i=2,\ldots,5), \tag{A.4}$$

$$\left(D^2+\frac{c_6}{m_6}\cdot D+\frac{k_6}{m_6}\right)\cdot\psi_6-\left(\frac{c_6}{m_6}\cdot D+\frac{k_6}{m_6}\right)\cdot\psi_5=0. \tag{A.5}$$

By solving Eqs. (A.1), (A.2) for x_6 as a function of x_0 gives

$$x_6\left(1-\frac{A_5G}{B_5H}+\frac{C_5B_4G}{B_5I_4H}\right)=-\frac{C_5C_4C_3C_2C_1}{B_5I_4I_3(A_2A_1-C_2B_1)}x_0 \tag{A.6}$$

with

$$I_3=A_3-\frac{C_3B_2A_1}{A_2A_1-C_2B_1},\quad I_4=A_4-\frac{C_4B_3}{I_3}. \tag{A.7}$$

The proper manipulation of Eqs. (A.3)–(A.5) also gives

$$x_0=-\frac{B_5I_4I_3(A_2A_1-C_2B_1)}{C_5C_4C_3C_2}\left(1-\frac{A_5G}{B_5H}+\frac{C_5B_4G}{B_5I_4H}\right)\psi_6. \tag{A.8}$$

Substituting Eq. (A.8) into Eq. (A.6) leads to the desired result for the 6th storey, i.e.

$$x_6=C_1\cdot\psi_6\implies x_6=\frac{c_1}{m_1}\dot{\psi}_6+\frac{k_1}{m_1}\psi_6. \tag{A.9}$$

Corresponding results [in the form of Eq. (9)] are obtained for each one of the remaining storeys by following the corresponding substitutions.

References

[1] J.T.P. Yao, Identification of structural damage in civil engineering, in: H.G. Natke (Ed.), *Application of System Identification in Engineering*, Springer, Berlin, 1988, pp. 349–390.

[2] G. De Roeck, The state-of-the-art of damage detection by vibration monitoring: the SIMCES experience, *Journal of Structural Control* 10 (2003) 127–134.

[3] A. Rytter, Vibration Based Inspection of Civil Engineering Structures, PhD Dissertation, Department of Building Technology and Structural Engineering, Aalborg University, Denmark, 1993.

[4] A.S. Kiremidjian, E.G. Straser, T. Meng, K. Law, H. Sohn, Structural damage monitoring for civil structures, *Proceedings of the International Workshop on Structural Health Monitoring*, Stanford, CA, 1997.

[5] S.W. Doebling, C.R. Farrar, M.B. Prime, D.W. Shevitz, Damage identification and health monitoring of structural and mechanical systems from changes in their vibration characteristics: a literature review, Report LA-13070-MS, Los Alamos National Laboratory, USA, 1996.

[6] Y. Zou, L. Tong, G.P. Steven, Vibration-based model-dependent damage (delamination) identification and health monitoring for composite structures—a review, *Journal of Sound and Vibration* 230 (2) (2000) 357–378.

[7] J.E. Mottershead, M.I. Friswell, Model updating in structural dynamics: a survey, *Journal of Sound and Vibration* 167 (2) (1993) 347–375.

[8] P. Hajela, F.J. Soeiro, Structural damage detection based on static and modal analysis, *AIAA Journal* 28 (1989) 110–115.

[9] E.A. Johnson, H.F. Lam, L.S. Katafygiotis, J.L. Beck, Phase I IASC-ASCE structural health monitoring benchmark problem using simulated data, *Journal of Engineering Mechanics* 130 (1) (2004) 3–15.

[10] H.F. Lam, L.S. Katafygiotis, N.C. Mickleborough, Application of a statistical model updating approach on phase I of the IASC-ASCE structural health monitoring benchmark study, *Journal of Engineering Mechanics* 130 (1) (2004) 34–48.

[11] C.R. Farrar, S.W. Doebling, An overview of modal-based damage identification methods, *Proceedings of DAMAS Conference*, Sheffield, UK, 1997.

[12] G. Hearn, R.B. Testa, Modal analysis for damage detection in structures, *Journal of Structural Engineering* 117 (1991) 3042–3063.

[13] D. Capecchi, F. Vestroni, Monitoring of structural systems by using frequency data, *Earthquake Engineering and Structural Dynamics* 28 (1999) 447–461.

[14] H.F. Lam, J.M. Ko, C.W. Wong, Localization of damaged structural connections based on experimental modal and sensitivity analysis, *Journal of Sound and Vibration* 210 (1) (1998) 91–115.

[15] C.G. Koh, L.M. See, Damage detection of buildings: numerical and experimental studies, *Journal of Structural Engineering* 121 (8) (1995) 1155–1160.

[16] M.H. Sadeghi, S.D. Fassois, A geometric approach to the non-destructive identification of faults in stochastic structural systems, *AIAA Journal* 35 (1997) 700–705.

[17] O.S. Salawu, Detection of structural damage through changes in frequency: a review, *Engineering Structures* 19 (1997) 718–723.

[18] M. Basseville, A. Benveniste, G. Moustakides, Detection and diagnosis of abrupt changes in modal characteristics of nonstationary digital signals, *IEEE Transactions Information Theory* 32 (3) (1986) 412–417.

[19] M. Basseville, M. Abdelghani, A. Benveniste, Subspace-based fault detection algorithms for vibration monitoring, *Automatica* 36 (1) (2000) 101–109.
[20] M. Nakamura, S.F. Masri, A.G. Chassiakos, T.K. Caughey, A method for non-parametric damage detection through the use of neural networks, *Earthquake Engineering and Structural Dynamics* 27 (1998) 997–1010.
[21] S.F. Masri, A.W. Smyth, A.G. Chassiakos, T.K. Caughey, N.F. Hunter, Application of neural networks for detection of changes in nonlinear systems, *ASCE Journal of Engineering Mechanics* 126 (7) (2000) 666–676.
[22] C.S. Huang, S.L. Hung, C.M. Wen, T.T. Tu, A neural network approach for structural identification and diagnosis of a building from seismic response data, *Earthquake Engineering and Structural Dynamics* 32 (2003) 187–206.
[23] A. Hera, Z. Hou, Application of wavelet approach for ASCE structural health monitoring benchmark studies, *Journal of Engineering Mechanics* 130 (1) (2004) 96–104.
[24] W.J. Staszeswski, Structural and mechanical damage detection using wavelets, *The Shock and Vibration Digest* 30 (6) (1998) 457–472.
[25] Z. Hou, M. Noori, R.St. Amand, Wavelet-based approach for structural damage detection, *Journal of Engineering Mechanics* 126 (7) (2000) 677–683.
[26] E. Cosenza, G. Manfredi, Damage indices and damage measures, *Progress in Structural Engineering and Materials* 2 (1) (2000) 50–59.
[27] E. DiPasquale, A.S. Cakmak, Detection of seismic structural damage using parameter-based global damage indices, *Probabilistic Engineering Mechanics* 5 (1990) 60–65.
[28] M.S. Williams, R.G. Sexsmith, Seismic damage indices for concrete structures: a state-of-the-art review, *Earthquake Spectra* 11 (1995) 319–349.
[29] G.V. Garcia, R. Osegueda, D. Meza, Damage detection comparison between damage index method and ARMA method, *Proceedings of International Modal Analysis Conference* 1 (1999) 593–598.
[30] P. Fajfar, P. Gaspersic, N2 method for the seismic damage analysis of RC buildings, *Earthquake Engineering and Structural Dynamics* 25 (1) (1996) 31–46.
[31] C.H. Loh, C.S. Hwang, W.Y. Jean, Seismic demand based on damage control model—considering basin effect and source effect, *Soil Dynamics and Earthquake Engineering* 17 (5) (1998) 335–345.
[32] S.D. Fassois, J.S. Sakellariou, Time series methods for fault detection and identification in vibrating structures, *Philosophical Transactions of the Royal Society*: *Mathematical*, *Physical and Engineering Sciences* (2006) invited paper, to appear.
[33] J.W. Lee, J.D. Kim, Health-monitoring method for bridges under ordinary traffic loadings, *Journal of Sound and Vibration* 257 (2) (2002) 247–264.
[34] J.S. Owen, B.J. Eccles, B.S. Choo, M.A. Woodings, The application of auto-regressive time-series modelling for the time–frequency analysis of civil engineering structures, *Engineering Structures* 23 (2001) 521–536.
[35] G.N. Fouskitakis, S.D. Fassois, Functional series TARMA modeling and simulation of earthquake ground motion, *Earthquake Engineering and Structural Dynamics* 31 (2) (2002) 399–420.
[36] L. Ljung, *System Identification: Theory for the User*, second ed., Prentice-Hall, Englewood Cliffs, NJ, 1999.
[37] S.D. Fassois, Parametric identification of vibrating structures, in: S.G. Braun, D.J. Ewins, S.S. Rao (Eds.), *Encyclopedia of Vibration*, Academic Press, New York, 2001.
[38] M.H. Sadeghi, S.D. Fassois, Reduced-dimensionality geometric approach to fault identification in stochastic structural systems, *AIAA Journal* 36 (1998) 2250–2256.
[39] L. Meirovitch, *Elements of Vibration Analysis*, second ed., McGraw-Hill, New York, 1986.
[40] D. Hudson, Reading and interpreting strong motion accelerograms, California Institute of Technology, 1979, pp. 49–54.
[41] D. Petrovski, N. Naumovski, *Processing of Strong Motion Accelerograms*: *Part I—Analytical Methods*, Institute of Earthquake Engineering and Engineering Seismology, University Kiril and Metodij, Skopje, 1979, Publication No. 66, pp. 15–17, 41–48.
[42] L. Cohen, *Time– Frequency Analysis*, Prentice-Hall, Englewood Cliffs, NJ, 1995.
[43] J.E. Lee, S.D. Fassois, On the problem of stochastic experimental modal analysis based on multiple-excitation multiple-response data—parts I and II, *Journal of Sound and Vibration* 161 (1993) 33–87.
[44] E.R. Dougherty, *Probability and Statistics for the Engineering, Computing and Physical Sciences*, Prentice-Hall, Englewood Cliffs, NJ, 1990.
[45] A. Cohen, *Biomedical Signal Processing—Vol. II*: *Compression and Automatic Recognition*, CRC Press, Boca Raton, 1988.
[46] J.S. Sakellariou, S.D. Fassois, Fault detection and identification in a scale aircraft skeleton structure via a functional model based method, 2006, submitted for publication.